processes

MDPI

Article

Development of a Continuous Process Chain for Selective Recovery and Purification of Rare Metals

Timo Dobler [1,*], Simon Buchheiser [1], Thomas Gaschler [2], Stefan Platzk [2], Harald Kruggel-Emden [2], Hermann Nirschl [1] and Marco Gleiß [1]

[1] Institute of Mechanical Process Engineering and Mechanics, Karlsruhe Institute of Technology (KIT), Strasse am Forum 8, 76131 Karlsruhe, Germany
[2] Chair of Mechanical Process Engineering and Solids Processing, Technische Universität Berlin, Ernst-Reuter-Platz 1, 10623 Berlin, Germany
* Correspondence: timo.dobler@kit.edu; Tel.: +49-721-608-44136

Abstract: Solar cells, liquid crystal displays (LCDs) and light-emitting diodes (LEDs) have become more and more important in recent decades. Crucial components of such electronic devices include rare metals (e.g., indium and gallium), which are only available in limited quantities. In order to meet their rising demand in the coming years, recycling processes, especially those that enable selective recovery of the individual components, are steadily gaining in importance. One conceivable method is particle-loaded solvent extraction followed by mechanical processing. Therefore, we first investigated the possibility of recovering individual particle fractions from a multicomponent mixture on the basis of the surface properties. Both UV–Vis spectroscopy and small-angle X-ray scattering (WAXS) were used for evaluation. The conducted experiments showed, among other things, that the indium oxide content increased from 50% to 99% in a binary system and from 33% to 94% in a ternary compound. In addition, the purification of the separated particles was examined in detail. Using UV–Vis spectrometry, it was found that permeation washing of filter cakes is suitable for removing impurities and retrieving most of the solvent used. Based on the results of the conducted laboratory tests, we finally developed a concept for the continuous and selective recovery of rare metals.

Keywords: recovery; solvent extraction; purification; filtration; cake washing; process design

Citation: Dobler, T.; Buchheiser, S.; Gaschler, T.; Platzk, S.; Kruggel-Emden, H.; Nirschl, H.; Gleiß, M. Development of a Continuous Process Chain for Selective Recovery and Purification of Rare Metals. *Processes* **2023**, *11*, 1847. https://doi.org/10.3390/pr11061847

Academic Editor: Anna Wołowicz

Received: 25 May 2023
Revised: 14 June 2023
Accepted: 16 June 2023
Published: 19 June 2023

1. Introduction

The development of technologies is growing at a fast rate. New products are becoming increasingly complex and are made up of many different components, such as base and rare metals [1]. Indium and gallium are two typical rare elements used in trace amounts in numerous electric devices, and are important due to their unique physical and chemical properties [2,3]. Solar cells, solders, semiconductors, light-emitting diodes (LEDs) and liquid crystal displays (LCDs) are some examples of products containing these critical components [2].

Due to the wide and steadily growing field of applications, the demand is rising as well [2,3]. Data released by the U.S. Geological Survey show that annual production of indium has increased from 220 to 900 tons and that of gallium from 100 to 550 tons since 2000 [4,5]. However, the long-term supply of these metals is problematic owing to their geological reserves, political constraints and huge request [6]. Both metals are rare, as gallium has a concentration of 0.0017% and indium 0.000005% in Earth's crust [7]. They are also found in very specific geographical regions. For example, China was responsible for 98% of the world's gallium and for 59% of the worldwide indium production in 2022 [5]. The availability can thus be affected by political interruptions, local disasters or conflicts of interest. Besides exploration of new mines and minimization of losses during processing, recycling of waste electrical and electronic equipment (WEEE) is one way to reduce the occurring supply risks [3,8].

Although the recycling rates are still low so far, some approaches for recovering indium and gallium from WEEE are described in the literature. Nagy et al. [9] and Swain et al. [10] used a combination of mechanical and chemical–thermal treatment to reclaim gallium from LEDs. Zhan et al. [11] showed that gallium with a purity of 92.8% can be recovered from LEDs by pyrolysis, physical disintegration and vacuum metallurgy. Virolainen et al. [12] employed acid leaching followed by solvent extraction to separate indium from indium tin oxide. La Torre et al. [13], Fontana et al. [14], Yang et al. [15] and Pereira et al. [16] adapted this method and demonstrated its applicability to LCD and front panel display recycling. In another study, Yang et al. [17] demonstrated that indium can be retrieved from LCD glass. Here, the authors achieved a purity of 90%.

However, the chemical decomposition required for solvent extraction is very time-consuming and costly [13,15]. Hence, particle-loaded solvent extraction based on the surface properties and without leaching is a conceivable alternative. For this purpose, WEEE is first pretreated by dismantling and shredding [18]. The crushed waste then endures high-temperature processes in which target materials such as base and precious metals are concentrated in a molten metal phase, while impurities and critical element oxides are transferred to a slag phase [18,19]. Next, this slag is comminuted until only primary particles remain. These particles are then fractionated by liquid–liquid extraction, whereby the product is enriched and collected in the organic solvent phase. Subsequently, the concentrated target suspension is filtered and washed, whereas the solvent is recycled for further use. Finally, the value particles are dewatered and dried to obtain a pure solid powder.

The focus of this publication is initially on the proof-of-concept of the described methodology. For this purpose, we start with single-substance extraction experiments to determine suitable process conditions. Based on this, multicomponent mixtures consisting of indium oxide, gallium oxide and silica are separated. Then, the captured particles are washed to remove any impurities and to retrieve the solvent utilized. From the results of these laboratory tests, we design a continuous process chain for the selective recovery of rare elements from solidified metal slag.

2. Materials and Methods

2.1. Particle System

The material systems used are gallium oxide (>99.99%, Carl Roth GmbH, Karlsruhe, Germany), indium oxide (>99.999%, Carl Roth GmbH, Germany) and silica (Quarzwerke GmbH, Haltern am See, Germany). The corresponding particle size distributions determined by laser diffraction (Sympatec GmbH, Clausthal-Zellerfeld, Germany) are given in Figure 1.

2.2. Liquid–Liquid Extraction

Fractionation and concentration are carried out by particle-loaded liquid–liquid extraction. Here, particles located initially in an aqueous subphase (BOT) are transported into an organic phase (TOP) after mixing of the two phases [20]. Essential for the separation success is the affinity of the target component to the top phase, which in turn is strongly related to the hydrophobicity of the particle surface. In principle, hydrophobic particles accumulate in the organic phase, while hydrophilic substances prefer an aqueous regime.

To influence the hydrophobicity of a system, it is possible to use collectors. These molecules consist of a nonpolar tail and a polar head, the latter being responsible for the linkage to the particle. Whether this linkage occurs and, if so, how strong the resulting bonds are depend on the charges of the head and the particle surface. If they have the same polarity, the strength of binding decreases as the charge difference rises. In case collector and particles have different loads, there is an enhanced adhesion of collector molecules to the surface and thus hydrophobization of the particles.

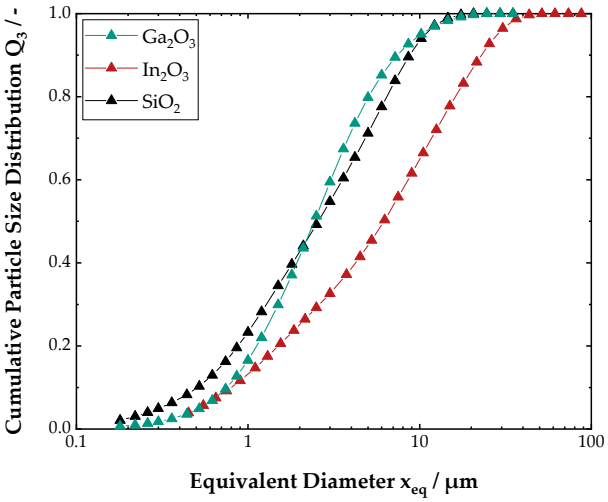

Figure 1. Particle size distribution of gallium oxide, indium oxide and silica. It is noticeable that the three material systems are all in a similar size range and have comparable distribution widths, which in turn justifies the assumption of prior comminution.

2.2.1. Experimental Procedure

The basis for all experiments are a 5 mL bottom phase and a 1 mL top phase. As the top phase, we employ 1-octanol (Carl Roth GmbH & Co. KG, Karlsruhe, Germany). The bottom phase consists of ultrapure water, hydrochloric acid (Carl Roth GmbH & Co. KG, Germany) or sodium hydroxide (VWR International GmbH, Darmstadt, Germany) along with metal oxide and, optionally, collector molecules. In the scope of this publication, cinnamic acid (Merck Chemicals GmbH, Darmstadt, Germany) and di-(2-ethylhexyl) phosphoric acid (Merck Chemicals GmbH, Germany) are used as collectors.

The preparation of the bottom phase proceeds as follows: First, metal oxide and collector suspensions with concentrations of 50 g/L and 0.5 g/L, respectively, are produced and ultrasonicated for 10 min. This ensures that existing agglomerates break up and that only primary particles are present. Subsequently, 4 mL of each suspension is placed in a snap-on lid bottle and made up to 10 mL either with ultrapure water, sodium hydroxide or hydrochloric acid, depending on the desired pH value. For the experiments without collectors, ultrapure water instead of collector suspension is applied. As a result, we obtain slurries with a solids content of 2 wt-% and a collector concentration of 0 or 10 kg/ton of metal oxide.

The suspension is then stirred for 10 min, causing intense blending of all components. Afterwards, 5 mL is taken as a reference sample. The remaining bottom phase is added with 1 mL of 1-octanol and both layers are mixed in a rotary blender for another 10 min. After the two phases have separated, we analyze the bottom phase using UV–Vis spectroscopy. Therefore, the absorption at a wavelength of 600 nm is measured and converted into a concentration by applying Lambert–Beer's law. In accordance with the same principle, the reference sample is characterized. The extraction process is shown schematically in Figure 2.

If the initial metal oxide suspension consists of several constituents, the composition of the top phase is also determined. For this purpose, it is separated into its solid and liquid parts by means of a laboratory nutsche. The particles remaining on the filter medium (Pall GmbH, Dreieich, Germany) are then dried and analyzed using wide-angle X-ray scattering (WAXS).

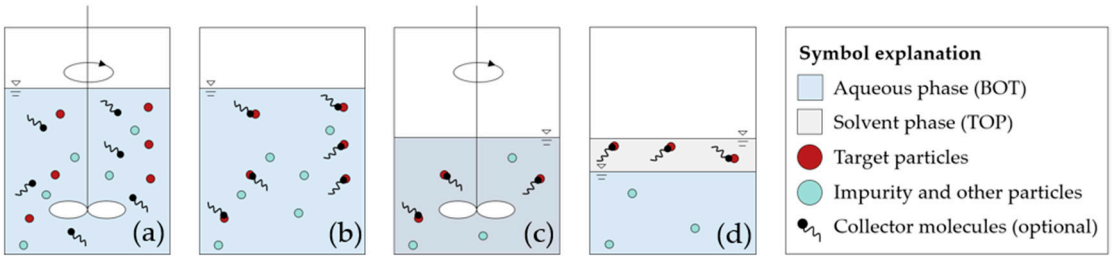

Figure 2. Schematic representation of the particle-loaded extraction process. First, an aqueous solution consisting of particles and collector molecules is prepared (**a**). Intensive stirring adsorbs the collector molecules to the surface of the valuable particles and increases their hydrophobicity (**b**). After taking a reference sample, a solvent phase is added and mixed with the aqueous subphase (**c**). Following phase separation, the hydrophobized target particles remain in the solvent together with the adsorbed collector molecules, while the other components still reside in the bottom phase (**d**).

2.2.2. Test Evaluation

The characterization of the single-substance extraction experiments are performed by determining the separation efficiency E. Therefore, the initial and final particle concentrations of the bottom phase ($c_{BOT,0}$ and $c_{BOT,t}$) obtained by UV–Vis spectrometry (UV-1900, Shimadzu Deutschland GmbH, Duisburg, Germany) are related to each other, yielding values between 0 (no deposition) and 1 (complete deposition). The following applies:

$$E = 1 - \frac{c_{BOT,t}}{c_{BOT,0}}. \tag{1}$$

Based on the detected separation efficiency E, we are able to calculate the selectivity S in a multicomponent system. It indicates the theoretical proportion of the target component i in a mixture consisting of i and j.

$$S_i = \frac{E_i}{E_i + \sum E_j} \tag{2}$$

However, this parameter is insufficient to quantify the actual separation result, since in reality particles influence and interact with each other. Here, an analysis of the upper phase is helpful. Possible characterization methods are, among others, X-ray photoelectron spectroscopy (XPS) [21], FT-IR spectroscopy [22,23] and wide angle X-ray scattering (WAXS), whereas we use the latter in this publication.

Therefore, the sample is irradiated with X-rays. Once the substance is crystalline, the beams are reflected at the lattice's reticular planes, which in turn leads to a diffraction pattern with material-specific Bragg peaks. In case all components of a mixture are crystalline, it is possible to calculate its composition from the ratio of the intensity of these characteristic peaks [24,25].

For this purpose, spectra of the pure components (see Figure 3) are recorded first. From these, a characteristic peak CP is determined for each substance, to be chosen so that there is no overlap between the systems used (here, gallium oxide at $2\theta = 31.8°$, indium oxide at $2\theta = 50.8°$ and silica at $2\theta = 26.6°$).

In the following, binary mixtures of a known composition (consisting of the value component i and one other component j) are measured and evaluated by means of the software Profex 5.1.1 [26]. A graphical plot of the intensity ratio $I_{CP,i}/I_{CP,j}$ as a function of the mass fraction m_i/m_j yields the linear regression curve

$$\frac{I_{CP,i}}{I_{CP,j}} = a_{i/j}\frac{m_i}{m_j} \tag{3}$$

for each mixture (see Figure 4). Based on the received data, the material system-specific proportionality constant $a_{i/j}$ is determinable and the mass fraction of a component i in an arbitrary system (made up of i and any number of j) may be calculated according to

$$\frac{m_i}{m_{tot}} = \frac{m_i}{m_i + \sum m_j} = \frac{1}{1 + \sum a_{i/j} \frac{I_{CP,j}}{I_{CP,i}}}. \quad (4)$$

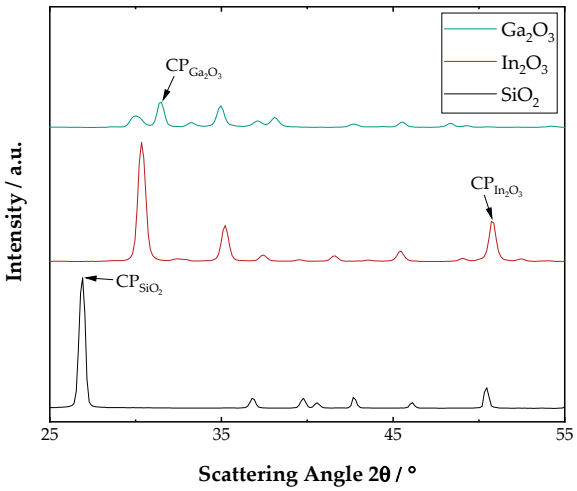

Figure 3. Scattering curves of the applied metal oxides. The characteristic peaks are at $2\theta = 31.8°$, $2\theta = 50.8°$ and $2\theta = 26.6°$.

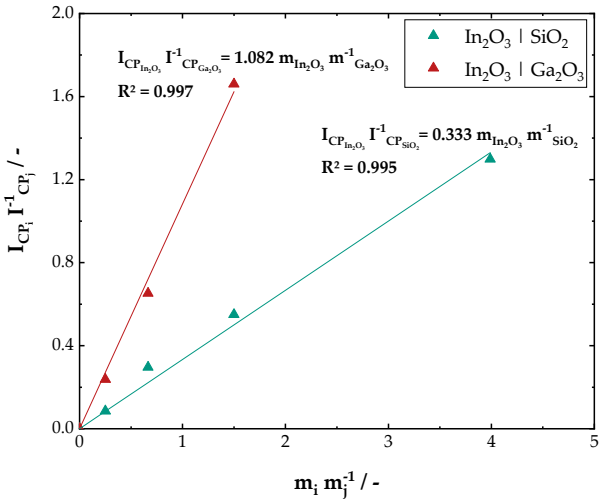

Figure 4. Intensity ratio as a function of the composition of the mixture. The material-specific proportionality constant $a_{i/j}$ can be determined by a linear fit.

The constants $a_{i/j}$ relevant for this work can be found in Table 1.

Table 1. System-specific proportionality constant and its coefficient of determination.

Mixture (i/j)	Proportionality Constant $a_{i/j}$/-	R-Square/-
In_2O_3/SiO_2	0.333	0.995
In_2O_3/Ga_2O_3	1.082	0.997

2.3. Cake Washing

After liquid–liquid extraction, the metal oxide particles and the collector molecules are located in a solvent phase. To isolate the valuable metal oxide and at the same time

retain as much solvent as possible, we filter the suspension and wash the remaining cake. Hence, this fulfills two important aspects:

(1) Removal of the collector molecules adsorbed on the particle surface;
(2) Recovery of the applied solvent.

2.3.1. Experimental Procedure

The basis for the tests is 30 mL of loaded top phase (here, indium oxide as particle system and di-(2-ethylhexyl) phosphoric acid as collector) prepared according to the methodology described in Section 2.2.1. This suspension is separated into its solid and liquid components using a laboratory nutsche with a filter area of 314 mm^2 and a pressure difference of 500 mbar. The filtrate is collected in a container, whereas the solid remains on a monophilic, solvent-resistant filter medium (SAATI Deutschland GmbH, Raesfeld, Germany) and forms a filter cake.

Next, the resulting cake is washed. Within the scope of this work, this is conducted by either a permeation or a dilution wash. Since both the collector [27] and the solvent are soluble in ethanol, ethyl alcohol is used as the washing liquid.

The permeation wash is carried out as follows: First, we carefully add 1 mL of ethanol to the cake surface. By applying a pressure difference of 500 mbar, it enters the cake, dissolves the collector, and displaces the solvent. The obtained filtrate is collected in a container and characterized by UV–Vis spectroscopy. Subsequently, the tank is emptied and thoroughly cleaned. The dilution wash procedure is almost identical, except that the applied washing liquid (single stage: 1 × 10 mL, two stage: 2 × 5 mL, three stage: 3 × 3.33 mL) and cake are mixed with each other. Hence, a suspension of particles, mother liquor and washing agent is formed. Analogous to the permeation experiments, this is separated at a pressure difference of 500 mbar and the produced filtrate is analyzed using UV–Vis spectroscopy.

Once the washing is complete, the filtrate stream can be divided into 1-octanol, collector and ethanol by distillation, allowing the pure components to be recirculated into the process.

2.3.2. Test Evaluation

The experiments are evaluated with UV–Vis spectroscopy (UV-1900, Shimadzu Deutschland GmbH, Germany). Using this method, the absorption is measured at a wavelength of 274 nm (peak of ethanol) and subsequently converted into a concentration c.

To characterize the washing process, we plot the concentration ratio c/c_0 (c_0 corresponds to the initial concentration) as a function of the wash ratio W

$$W = \frac{V_{WL}}{V_P} = \frac{V_{WL}}{\varepsilon V_C}. \tag{5}$$

This parameter links the volume of the washing liquid V_{WL} and the pore volume of the filter cake V_P, although the latter could be expressed by the cake volume V_C and the gravimetrically determined porosity ε. Assuming that the filter cake is completely saturated with liquid after the washing process, the porosity is calculated as

$$\varepsilon = \frac{(m_{C,wet} - m_C)/\rho_L}{(m_{C,wet} - m_C)/\rho_L + m_C/\rho_S}, \tag{6}$$

where ρ_L and ρ_S represent the densities of the fluid and solid, and $m_{C,wet}$ as well as m_C are the masses before and after thermal drying at 100 °C.

3. Results and Discussion

In the following chapter, the results of the experiments are presented and discussed. First, the focus is on the selective fractionation of multicomponent systems by a particle-loaded liquid–liquid extraction. For this purpose, single-substance tests are carried out to

select a suitable collector and to determine appropriate operating conditions. Subsequently, binary and ternary mixtures are separated, isolating indium oxide from the other components. After fractionation, the target particles and the collector molecules are present in a solvent phase. To finally obtain the value product, we filtrate the suspension and wash the remaining cake.

3.1. Liquid–Liquid Extraction

3.1.1. Single-System Extraction

The aim of the extraction step is to separate a mixture of several components as selectively as possible into its individual constituents. For this purpose, the experimental conditions are ideally selected in the way that only one substance system is transported into the upper phase, while all other particles remain in the lower phase. To determine suitable process parameters, we first perform single-substance extraction experiments and investigate the influence of the collector molecule and the pH level on the separation performance. Figure 5 shows the data obtained for indium oxide (a) and gallium oxide (b). Since the separation rate is zero for silica both without and with the collector at all relevant pH values, the results for this system are not explicitly depicted here.

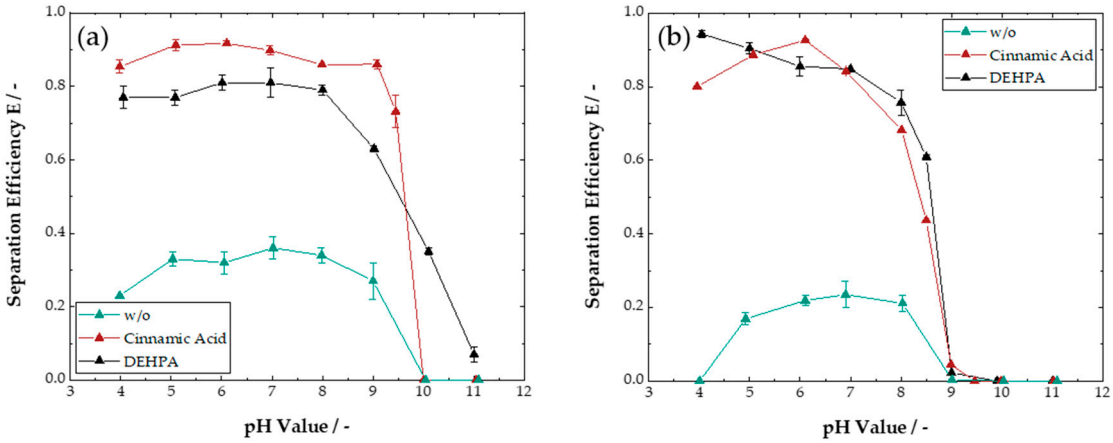

Figure 5. Influence of the collector molecule on the separation efficiency of (**a**) indium and (**b**) gallium oxide. For both substance systems, it can be seen that the presence of a collector significantly increases the deposition performance. It is also noticeable that the collector selection has an almost negligible influence on the separation result when applying gallium oxide in the experiments carried out, whereas there is a clear dependence on the collector molecule when using indium oxide.

Figure 5 indicates that the separation efficiency of both metal oxides is comparatively low in the absence of a collector (w/o). Here, maximum deposition values of 36% for indium oxide (a) and 23% for gallium oxide (b) can be reached. However, the behavior changes after adding collector molecules. For both cinnamic acid and di-(2-ethylhexyl) phosphoric acid (DEHPA), we then obtain significantly higher separation rates of up to 92% and 94%, respectively. The main reason for this is the hydrophobicity of the particle surface. Initially, the hydrophilic parts predominate, leading to an increased affinity to the aqueous subphase. Due to the addition of the collector molecules, the surfaces of the metal oxides become more hydrophobic, which in turn causes an enhanced affinity to the upper phase and consequently improves the degree of separation.

The figure also demonstrates that the separation efficiency is a function of the pH value and of the applied collector. Up to a certain pH level, comparatively high separation rates for indium oxide (a) as well as for gallium oxide (b) are recognizable. However, if that pH is exceeded, there is a rapid drop in the curves. For indium oxide (a), this occurs at pH 8 to 9, depending on the collector used, whereas for gallium oxide (b) it starts at lower pH values, and is independent of the collector. To understand the phenomenon, it is helpful to look at the chemical structure of the collector molecules used. Cinnamic acid and DEHPA

are anionic collectors, since their head is a carboxy or alkyl phosphate residue [27,28]. Hence, there is primarily adsorption to positively charged particle surfaces. However, with increasing pH the surface charge of indium and gallium oxide declines steadily, which is why the binding force between particle and collector also decreases successively. Analogously, it is possible to explain why no separation whatsoever is detectable in the case of constantly negatively charged silica [29].

In summary, the single-component experiments exhibit, on the one hand, that a collector is necessary for a successful deposition and, on the other hand, that the separation performance depends on the pH value of the bottom phase. Taking these aspects into account, it is feasible to derive suitable process parameters for the selective capture of indium oxide from a multicomponent system. Therefore, we calculate the collector-dependent theoretical indium content after the extraction step based on the determined separation efficiencies using Equation (2). Figure 6 shows the computed data for cinnamic acid (a) and DEHPA (b).

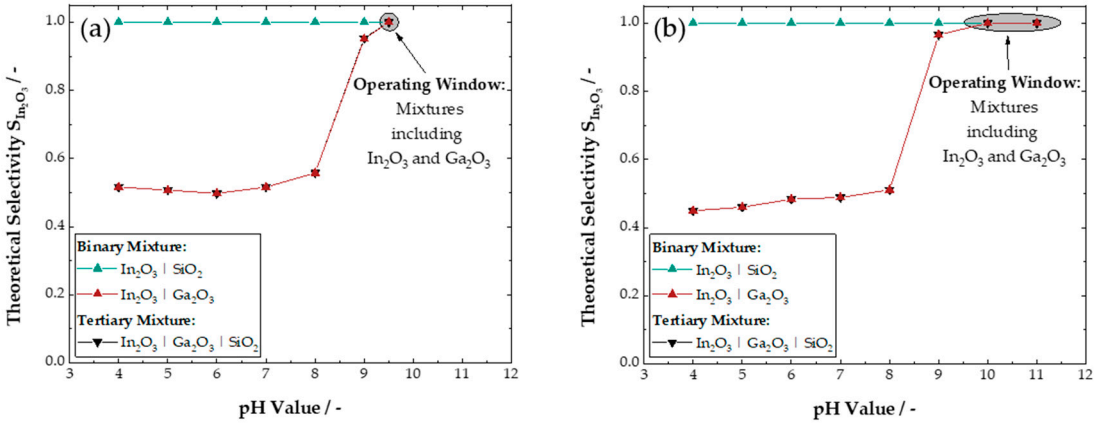

Figure 6. Theoretical calculated indium content in the top phase after liquid–liquid extraction. For (**a**) cinnamic acid and (**b**) DEHPA, the determined content in a binary mixture of silica and indium oxide is constant at 100%. With blends containing both indium oxide and gallium oxide, differences in the size of the operating window are visible.

For a binary mixture of indium oxide and silica, the selectivity for both collectors is constant at 100% within the investigated pH range. The lack of top phase affinity of silica leads to a wide operating window, covering the pH area between 4 and 9.5 for cinnamic acid and between 4 and 11 for DEHPA. To recover as much indium oxide as possible, it is advisable to fulfill the liquid–liquid extraction at the pH value with the highest separation efficiency, since the maximum yield is achieved at this point (here, pH = 6).

Once the mixture to be fractionated contains both indium and gallium oxide, the determination of ideal process parameters is more complicated. In this case, the selectivity is around 50% up to pH 8 before rising abruptly. Accordingly, a pH value in the alkaline range is required to achieve selective deposition of indium oxide. However, since the separation efficiency of the desired product also drops in this area, the operating window is comparatively small and limited to pH 9.5 for cinnamic acid (a) and between 10 and 11 for DEHPA (b).

3.1.2. Multi-System Extraction

The results of the single-substance experiments suggest that indium oxide can be separated selectively from a multicomponent mixture using cinnamic acid or DEHPA as the collector molecule. For this reason, we subsequently perform particle-loaded liquid–liquid extractions with binary and ternary mixtures. The process conditions chosen for the experiments are based on the theoretically determined selectivities (see Figure 6) and can be found in Table 2. The table also contains the mass ratios of the metal oxides used in the initial bottom phase.

Table 2. Experimental conditions for the multi-system extractions.

Collector	Mixture	pH Value	Composition BOT (wt %)
Cinnamic Acid	$In_2O_3SiO_2$	6	50 | 50
	In_2O_3 | Ga_2O_3	9.5	50 | 50
	In_2O_3 | Ga_2O_3 | SiO_2	9.5	33.3 | 33.3 | 33.3
DEHPA	In_2O_3 | SiO_2	6	50 | 50
	In_2O_3 | Ga_2O_3	10	50 | 50
	In_2O_3 | Ga_2O_3 | SiO_2	10	33.3 | 33.3 | 33.3

In Table 3, the theoretical and the real compositions of the top phase after extraction are shown. For binary systems of indium oxide and silica, there is a good agreement between theory and experiment regardless of the applied collector molecule. Here, the small amount of silica in the solvent phase is primarily due to the formation of heteroagglomerates between the negatively charged silica and the positively charged indium particles [30].

Table 3. Theoretical and real compositions of the top phase after multi-system extractions.

Collector	Mixture	Composition TOP (wt %)	
		Theoretical	Experimental
Cinnamic Acid	In_2O_3 | SiO_2	100 | 0	98.3 | 1.7
	In_2O_3 | Ga_2O_3	100 | 0	76.7 | 23.3
	In_2O_3 | Ga_2O_3 | SiO_2	100 | 0 | 0	74.2 | 13.9 | 11.9
DEHPA	In_2O_3 | SiO_2	100 | 0	98.9 | 1.1
	In_2O_3 | Ga_2O_3	100 | 0	93.1 | 6.9
	In_2O_3 | Ga_2O_3 | SiO_2	100 | 0 | 0	94.1 | 5.0 | 0.9

In the case of binary and ternary mixtures containing gallium and indium oxide, the difference between the calculated and actual composition is more visible, especially when cinnamic acid is used. These deviations are again caused by the formation of heteroagglomerates on the one hand and by the small operating window on the other hand. The latter ensures that a minor part of the added collector also adsorbs onto the surface of the gallium oxide, which in turn leads to an undesirable separation in the further course. However, this effect becomes less significant when applying DEHPA as collector. Since the experiments take place at a higher pH, the charge of the gallium oxide surface is already sufficiently negative here, resulting in limited interactions between the particles and the collector. As a result, the deposited fraction exhibits a high indium oxide content (up to 94.1%), which is in a similar range to the purities achieved by Yang et al. [15] and Zhan et al. [11] when recycling LCD glass and light-emitting diodes. These were 90 and 92.8%, respectively.

Overall, both the single-substance and the multi-substance experiments demonstrate that particle-loaded liquid–liquid extraction is basically suitable for fractionation of metal oxide mixtures, although the collector used is of particular importance.

3.2. Filter Cake Washing

Following extraction, the metal oxide particles and collector molecules adsorbed on their surface are present in an organic upper phase. To isolate the valuable product and recover as much as possible of the applied solvent, washing with ethanol takes place. The choice of this washing agent has two reasons; on the one hand, it is mixable with 1-octanol and, on the other hand, it exhibits a high collector solubility (100 mg/mL) [27]. The latter ensures that even at separation efficiencies of 100%, 0.291 mL (here, corresponding to a wash ratio of about 0.45) is sufficient to fully dissolve all collector molecules.

Once the collector has been washed out, the focus is on the recovery of the solvent. Therefore, permeation and dilution washing experiments take place. The results are shown in Figure 7.

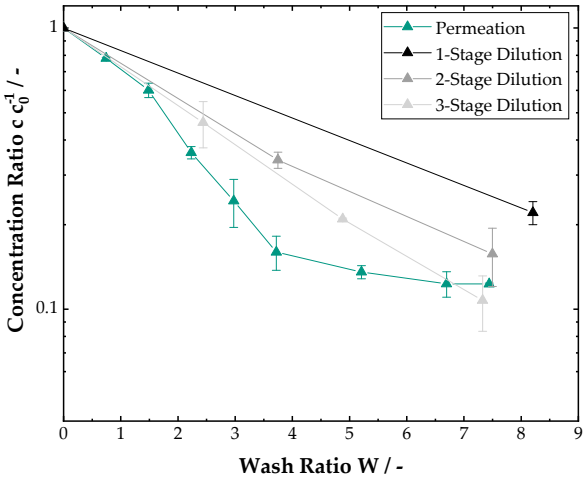

Figure 7. Washing results as a function of the washing liquid consumption and the type of washing.

The diagram suggests that the solvent content in the filter cake can be reduced significantly by both types of washing. For dilution wash, final concentration ratios between 11 and 22% are achievable, accompanied by a corresponding recovery rate of up to 89%. In this context, it is obvious that the higher the number of washing stages, the lower the solvent content remaining in the filter cake and the better the washing result. However, it should be noted that the complexity of the process also increases with the number of washing stages, thus complicating the technical implementation and rising the operating costs.

In comparison, permeation washing is easy to implement because it is based solely on the displacement of the mother liquor from the pores of the filter cake and does not entail resuspension of the components [31]. Unlike dilution, this type of washing reaches a state of equilibrium above a certain wash ratio, with the concentration level assuming a constant value due to back-mixing by dispersion and diffusion [32]. In the experiments carried out, this behavior is evident from a wash ratio of about 6.5. Here, the critical value is approximately 0.12 and thus close to the obtainable final concentration for three-stage dilution washing.

In summary, the tests reveal that both wash methods enable almost 90% of the solvent originally present in the filter cake to be recovered and subsequently returned to the process. With regard to the development of a continuous process chain and considering the apparatus effort, a permeation wash is to be preferred for the application discussed in this publication.

3.3. Continuous Process Chain

The executed experiments prove that the process chain consisting of comminution, liquid–liquid extraction and mechanical solid–liquid separation as outlined in Figure 8 is generally suitable for the selective separation of a solidified metal slag. Compared to existing recycling approaches, the elimination of chemical pretreatment prior to the extraction step is particularly advantageous, as it significantly reduces both resource requirements and process time while simultaneously enhancing throughput.

So far, the proof-of-concept took place in batch operation and on laboratory scale. Due to the promising results and with regard to the scalability of the concept, a transfer to continuous equipment is conceivable. A possible apparatus implementation of the resulting process chain is shown in Figure 9 and comprises a bead mill, an extraction cell and a belt filter.

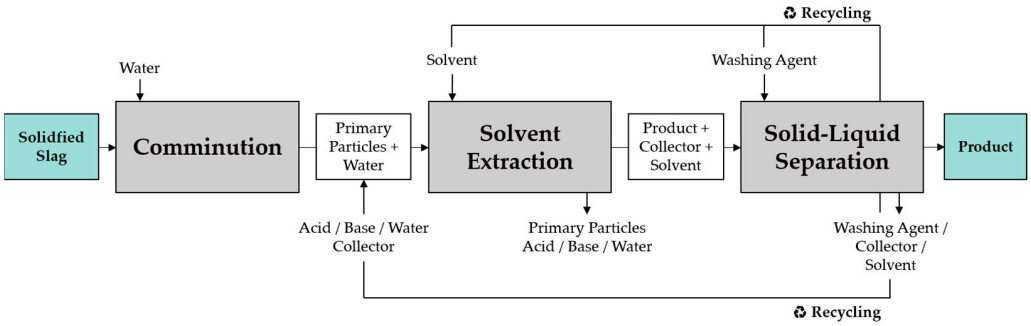

Figure 8. Process flow diagram. Initially, the slag is crushed into primary particles by wet comminution. After the addition of collector molecules and pH regulators, fractionation takes place by liquid–liquid extraction. Here, the valuable particles are transported in a solvent phase. The separated particles are finally purified and dehumidified so that there is only the dry product at the end of the process.

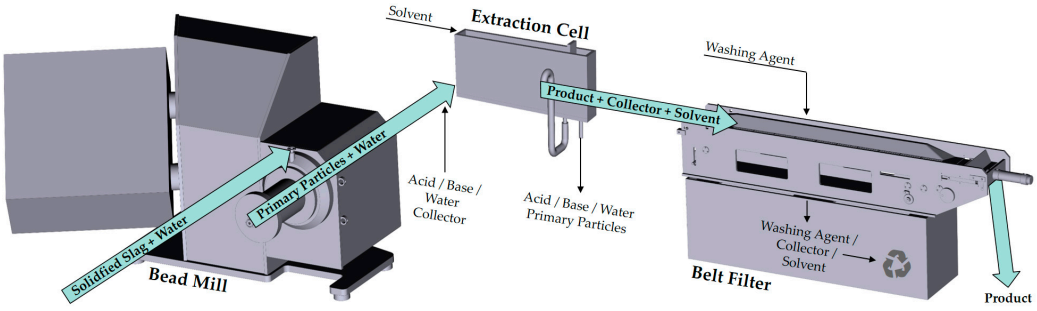

Figure 9. Modular process chain for the continuous and selective recovery of rare elements from solidified metal slag. The process chain consists of a bead mill, an extraction cell and a belt filter.

Bead Mill: Initially, the valuable particles and all other constituents are present as solidified metal slag. However, for selective separation of the components, primary particles are required. For this reason, the slag is comminuted in a bead mill. Therefore, a suspension consisting of slag and water is fed into a rotating drum filled with grinding media. The interaction between the material to be milled and the grinding media results in the input of shear and impact forces, which in turn crush the particles down to their primary size.

Extraction Cell: Next, fractionation of the primary particles takes place in a continuous extraction cell. Therefore, we adjust the pH of the suspension by injecting acid or base followed by adding the collector. The resulting slurry is then transferred to the extraction cell and mixed with the solvent. Upon phase separation, the valuable particles remain in the upper phase, while all other components stay in the aqueous lower phase and can be separated from each other by pH shifts and further extraction steps.

Belt Filter: Once fractionation is complete, the valuable product and collector molecules are dispersed in solvent. To isolate the rare element particles in their pure form and to recover the solvent as completely as possible, a filtration and subsequent washing process is recommended. Since the latter is comparatively intensive (see Section 3.2), we use a vacuum belt filter for this purpose. Apart from the filtration and washing, a thermal drying can also be implemented on this apparatus by means of minor instrumental adjustments [33], which in turn enables complete drying of the product.

4. Conclusions

To meet the rising demand for rare metals in the coming decades, recycling of waste electrical and electronic equipment becomes more and more important. One method often used in this context is pyrometallurgy. Here, the metallic components are liquefied by the addition of thermal energy, resulting in a molten and a slag phase. Although the latter contains, among other things, precious metal oxides, it has received only secondary

attention so far. Motivated to change this situation, we investigated the possibility of recovering the valuable components selectively from such a solidified metal slag.

For this purpose, particle-loaded liquid–liquid extraction experiments were carried out on laboratory scale. These demonstrated that both binary and ternary particle mixtures could be fractionated almost completely based solely on their surface properties, without the need for prior chemical leaching. The collector molecules required for this method could then be removed without residue by a subsequent washing process; thus, only the value product remained. Furthermore, this washing step allowed for a significant proportion of the solvent stream utilized in the extraction process to be retrieved. Based on the promising results of the performed laboratory tests, a continuous process chain was designed enabling fractionation and purification of solidified metal slag. Following commissioning and successful proof-of-concept, a scale-up to industrial level is envisaged.

Author Contributions: Conceptualization, T.D.; Data curation, T.D.; Formal analysis, T.D.; Funding acquisition, M.G.; Investigation, T.D., S.B. and T.G.; Methodology, T.D.; Project administration, H.N.; Supervision, H.K.-E., H.N. and M.G.; Validation, T.D.; Visualization, T.D.; Writing—original draft, T.D.; Writing—review and editing, T.D., S.B., T.G., S.P., H.K.-E., H.N. and M.G. All authors have read and agreed to the published version of the manuscript.

Funding: This research was funded by the German Research Foundation within the priority program SPP 2315 'Engineered Artificial Minerals' (Project number: 470336895).

Data Availability Statement: The data presented in this study are available on request from the corresponding author.

Conflicts of Interest: The authors have declared no conflicts of interest.

References

1. Andersson, M.; Ljunggren Söderman, M.; Sandén, B.A. Challenges of recycling multiple scarce metals: The case of Swedish ELV and WEEE recycling. *Resour. Policy* **2019**, *63*, 101403. [CrossRef]
2. Sinclar, W.D. Electronic Metals (In, Ge and Ga): Present and Future Resources. *Acta Geol. Sin.-Engl. Ed.* **2014**, *88*, 463–465. [CrossRef] [PubMed]
3. Zhang, S.; Ding, Y.; Liu, B.; Chang, C.-C. Supply and demand of some critical metals and present status of their recycling in WEEE. *Waste Manag.* **2017**, *65*, 113–127. [CrossRef] [PubMed]
4. U.S. Geological Survey. *Mineral Commodity Summaries 2001*.. Available online: https://www.usgs.gov/publications/mineral-commodity-summaries-2001 (accessed on 15 May 2023).
5. U.S. Geological Survey. *Mineral Commodity Summaries 2023*.. Available online: https://www.usgs.gov/publications/mineral-commodity-summaries-2023 (accessed on 15 May 2023).
6. Eggert, R.G. Minerals go critical. *Nat. Chem.* **2011**, *3*, 688–691. [CrossRef]
7. Redlinger, M.; Eggert, R.; Woodhouse, M. Evaluating the availability of gallium, indium, and tellurium from recycled photovoltaic modules. *Sol. Energy Mater. Sol. Cells* **2015**, *138*, 58–71. [CrossRef]
8. Licht, C.; Peiró, L.T.; Villalba, G. Global Substance Flow Analysis of Gallium, Germanium, and Indium: Quantification of Extraction, Uses, and Dissipative Losses within their Anthropogenic Cycles. *J. Ind. Ecol.* **2015**, *19*, 890–903. [CrossRef]
9. Nagy, S.; Bokányi, L.; Gombkötő, I.; Magyar, T. Recycling of Gallium from End-of-Life Light Emitting Diodes. *Arch. Metall. Mater.* **2017**, *62*, 1161–1166. [CrossRef]
10. Swain, B.; Mishra, C.; Kang, L.; Park, K.-S.; Lee, C.G.; Hong, H.S. Recycling process for recovery of gallium from GaN an e-waste of LED industry through ball milling, annealing and leaching. *Environ. Res.* **2015**, *138*, 401–408. [CrossRef]
11. Zhan, L.; Xia, F.; Ye, Q.; Xiang, X.; Xie, B. Novel recycle technology for recovering rare metals (Ga, In) from waste light-emitting diodes. *J. Hazard. Mater.* **2015**, *299*, 388–394. [CrossRef]
12. Virolainen, S.; Ibana, D.; Paatero, E. Recovery of indium from indium tin oxide by solvent extraction. *Hydrometallurgy* **2011**, *107*, 56–61. [CrossRef]
13. de La Torre, E.; Vargas, E.; Ron, C.; Gámez, S. Europium, Yttrium, and Indium Recovery from Electronic Wastes. *Metals* **2018**, *8*, 777. [CrossRef]
14. Fontana, D.; Forte, F.; de Carolis, R.; Grosso, M. Materials recovery from waste liquid crystal displays: A focus on indium. *Waste Manag.* **2015**, *45*, 325–333. [CrossRef] [PubMed]
15. Yang, J.; Retegan, T.; Steenari, B.-M.; Ekberg, C. Recovery of indium and yttrium from Flat Panel Display waste using solvent extraction. *Sep. Purif. Technol.* **2016**, *166*, 117–124. [CrossRef]
16. Pereira, E.B.; Suliman, A.L.; Tanabe, E.H.; Bertuol, D.A. Recovery of indium from liquid crystal displays of discarded mobile phones using solvent extraction. *Miner. Eng.* **2018**, *119*, 67–72. [CrossRef]

17. Yang, J.; Retegan, T.; Ekberg, C. Indium recovery from discarded LCD panel glass by solvent extraction. *Hydrometallurgy* **2013**, *137*, 68–77. [CrossRef]
18. Zhang, L.; Xu, Z. A review of current progress of recycling technologies for metals from waste electrical and electronic equipment. *J. Clean. Prod.* **2016**, *127*, 19–36. [CrossRef]
19. Ebin, B.; Isik, M.I. Pyrometallurgical Processes for the Recovery of Metals from WEEE. In *WEEE Recycling*; Elsevier: Amsterdam, The Netherlands, 2016; pp. 107–137.
20. Sawistowski, H. Physical Aspects of Liquid-Liquid Extraction. In *Mass Transfer with Chemical Reaction in Multiphase Systems. Alper, E., Ed.*; Springer Netherlands: Dordrecht, The Netherlands, 1983; pp. 613–635.
21. Kumar, A.; Negi, S.; Choudhury, T.; Mutreja, V.; Sunaina, S.; Sahoo, S.C.; Singh, A.; Mehta, S.K.; Kataria, R.; Saini, V. A highly sensitive and specific luminescent MOF determines nitric oxide production and quantifies hydrogen sulfide-mediated inhibition of nitric oxide in living cells. *Mikrochim. Acta* **2023**, *190*, 127. [CrossRef]
22. Kirandeep; Kaur, J.; Sharma, I.; Zangrando, E.; Pal, K.; Mehta, S.K.; Kataria, R. Fabrication of novel copper MOF nanoparticles for nanozymatic detection of mercury ions. *J. Mater. Res. Technol.* **2023**, *22*, 278–291. [CrossRef]
23. Kumar, A.; Mutreja, V.; Anand, V.; Mehta, S.K.; Zangrando, E.; Kataria, R. Solvent templated luminescent metal-organic frameworks for specific detection of vitamin C in aqueous media. *J. Mol. Struct.* **2023**, *1284*, 135365. [CrossRef]
24. Buchheiser, S.; Deutschmann, M.P.; Rhein, F.; Allmang, A.; Fedoryk, M.; Stelzner, B.; Harth, S.; Trimis, D.; Nirschl, H. Particle and Phase Analysis of Combusted Iron Particles for Energy Storage and Release. *Materials* **2023**, *16*, 2009. [CrossRef]
25. Hubbard, C.R.; Snyder, R.L. RIR-Measurement and Use in Quantitative XRD. *Powder Diffr.* **1988**, *3*, 74–77. [CrossRef]
26. Doebelin, N.; Kleeberg, R. Profex: A graphical user interface for the Rietveld refinement program BGMN. *J. Appl. Crystallogr.* **2015**, *48*, 1573–1580. [CrossRef] [PubMed]
27. Sigma-Aldrich. Bis-(2-ethylhexyl)-phosphorsäure. Available online: https://www.sigmaaldrich.com/US/en/product/aldrich/237825 (accessed on 15 May 2023).
28. Sigma-Aldrich. Cinnamic Acid. Available online: https://www.sigmaaldrich.com/US/en/substance/cinnamicacid14816140103 (accessed on 15 May 2023).
29. Rhein, F.; Schmid, E.; Esquivel, F.B.; Nirschl, H. Opportunities and Challenges of Magnetic Seeded Filtration in Multidimensional Fractionation. *Chem. Ing. Tech.* **2020**, *92*, 266–274. [CrossRef]
30. Cerbelaud, M.; Videcoq, A.; Abélard, P.; Ferrando, R. Simulation of the heteroagglomeration between highly size-asymmetric ceramic particles. *J. Colloid Interface Sci.* **2009**, *332*, 360–365. [CrossRef]
31. Anlauf, H. *Wet Cake Filtration: Fundamentals, Equipment, Strategies*; WILEY VCH: Weinheim, Germany, 2020.
32. Wilkens, M.; Peuker, U.A. Grundlagen und aktuelle Entwicklungen der Filterkuchenwaschung. *Chem. Ing. Tech.* **2012**, *84*, 1873–1884. [CrossRef]
33. Dobler, T.; Buchheiser, S.; Gleiß, M.; Nirschl, H. Development and Commissioning of a Small-Scale, Modular and Integrated Plant for the Quasi-Continuous Production of Crystalline Particles. *Processes* **2021**, *9*, 663. [CrossRef]